Online ISSN: 3005-7744

Optimizing Chrysin's Anticancer Efficacy on MDA-MB-231 Cells: Synthesis and Characterization of Chrysin-Loaded Gold/Chitosan Nanoparticles

Saja Hussain Dilfy⁰^{1,*}, Nawras Najah Mubark⁰², and Abiya Ahad³

^{*}Corresponding author name: Saja Hussain Dilfy, Email:gl1107@uowasit.edu.iq



ORIGINAL A R T I C L E

Received: 10.05.2023 **Revised:** 21.05.2023

Accepted: 26.05.2023 **DOI:** 10.57238/tpb.2023.144270.1001



ABSTRACT

This study showcases the creation of nanostructures that carry Chrysin (Chr), using gold (AuNPs) nanoparticles encased in chitosan. The Au particles were derived by reducing AuCl4 $^-$ with tripolyphosphate (TPP) and CS. These gold/chitosan nanoparticles (Au/CS NPs) were analyzed using UV-Vis spectroscopy. Their size was identified as approximately $45.23\pm4.32\,\mathrm{nm}$ through DLS, and the crystal makeup of gold was verified by XRD. FE-SEM imaging confirmed these NPs to be round, with an average size around $42\,\mathrm{nm}$. Measurements showed that the drug capacity for Chr was about $20\pm3.70\%$ and its encapsulation efficiency stood at roughly $88.7\pm4.50\%$. The nanocarrier's drug release behavior was observed in both acidic and neutral conditions (with pH levels of $5.4\,\mathrm{and}~7.4$), and it was notably responsive to the acidic environment. Moreover, MTT test showed the Chr-infused NPs were more toxic to the MDA-MB-231 breast cancer cells than Chr alone. Based on this data, further exploration of these Au/CS NPs is recommended to enhance the therapeutic potential of Chr.

Keywords: Drug delivery, Chrysin, Gold nanoparticles, Chitosan, Cytotoxicity.

1 INTRODUCTION

Ately, cancer has gained prominence as a leading cause of death and disease in many countries. Over Ithe past years, given the significant role of natural medicine in cancer therapy, numerous research efforts have centered on developing new methods to improve the delivery systems for natural compounds or extracts [1]. Chrysin (Chr) is a naturally occurring flavonoid found in various plants, including the blue passion flower (Passiflora caerulea) and honey. Over the years, it has garnered interest for its potential health benefits, including its potential anticancer properties. Chr has been shown to exert its anticancer effects through various mechanisms, such as inhibiting tumor cell proliferation, inducing apoptosis, inhibiting inflammation, and modulating certain enzyme activities and signaling pathways [2,3]. However, its effectiveness in cancer treatment is restricted due to its water-repelling characteristics, poor absorption, swift breakdown, and

fast metabolism. Using nanocarrier formulations can help address these challenges, such as its water insolubility and reduced therapeutic effectiveness [4,5]. Nanocarriers, particularly gold nanoparticles, have become noteworthy due to their distinctive properties such as low toxicity, stability, minimal cell harm, adjustable surface qualities, and biocompatibility [6]. Moreover, gold nanoparticles are actively studied for their use in cancer therapy using heat, as well as valuable tools for early detection and imaging [7]. Typically, these nanoparticles are combined with therapeutic substances to help them penetrate and stay within tumor blood vessels, leveraging the enhanced permeability and retention (EPR) effect. Only a select few therapeutic agents can directly bind to gold nanoparticles. Hence, it's crucial to develop new structures to enhance their drug delivery capacities, like carrying diverse cancer drugs. One solution could be coating gold nanoparticles

 $^{^{1}}$ Department of Biology, College of Education for Pure Science, University of Wasit, Wasit, 52001, Iraq.

²Department of Pathological Analyzes, College of Science, University of Wasit, Wasit, 52001, Iraq.

³Ananta Institute of Medical Sciences and Research Center AIMS-RC, Rajsamand, Udaipur, India.

with a polymer shell [8,9]. Bhumkar and colleagues developed gold nanoparticles reduced by chitosan for the transmucosal delivery of insulin [10]. Additionally, gold nanoparticles with a double-shell of poly-L-lysine have been utilized effectively as DNA carriers [11]. Chitosan (CS) is among the most prevalent biocompatible polymers globally, celebrated for its biodegradability and biocompatibility. Using CS as a coating for gold nanoparticles could enhance their drug delivery capabilities, particularly in drug loading and therapeutic effectiveness [12]. This study introduces the creation of a chrysin delivery mechanism using gold/chitosan nanoparticles (Au/CS NPs) that feature gold as the core and chitosan as the shell. After synthesizing the Au/CS NPs, they were infused with chrysin, resulting in Chr-Au/CS NPs, and their physical and chemical attributes were analyzed. The impact of these nanoparticles on the MDA-MB-231 breast cancer cells, as a highly aggressive, invasive and poorly differentiated triple-negative breast cancer cells, in terms of toxicity was evaluated using the MTT assay.

2 MATERIALS AND METHODS

2.1 Materials

Chitosan, with a molecular weight ranging from 10^5 to 3×10^5 g/mol and a degree of deacetylation of 75% or more, along with Tripolyphosphate (Na₅P₃O₁₀, TPP), 5-diphenyltetrazolium bromide (MTT), and Dimethyl sulfoxide (DMSO), were sourced from Sigma (St. Louis, MO, USA). The cell culture medium RPMI, Fetal Bovine Serum (FBS), and penicillin/streptomycin were acquired from Atocel Company (Budapest, Hungary). HAuCl₄ was provided by Acros Organics. Chrysin and all other solvents of the highest commercial quality were procured from Merck and were utilized as received, without additional purification.

2.2 Synthesis of Au/CS NPs

Before being used, all glass equipment was first cleansed in a 50% sulfuric acid solution and then rigorously rinsed with water. For the synthesis of the core-shell AuNPs, a TPP solution in water (0.1%) was introduced to a 0.5% CS solution (3 mL) while stirring magnetically. After a duration of 50 minutes, a water-based HAuCl4 solution (2 mL, 60 mM) was incorporated, the mixture's temperature was elevated to 70°C, and the stirring process was maintained for an additional 45 minutes.

2.3 Drug loading

The process for drug loading involved dissolving 2 mg of chr in 1 mL of DMSO, which was then combined with a 2 mL solution of Au/CS NPs. This mixture was stirred for 24 hours in a dark environment at ambient temperature.

After this, the Chr-infused Au/CS NPs were isolated using centrifugation at 14,000 rpm. These were then subjected to drying in a vacuum oven set at 30 °C for a duration of 12 hours. The amount of Chr present in the NPs was determined using a UV-Vis spectrophotometer, focusing on a wavelength of 267 nm. To deduce the drug-loading percentage (DL%) and the encapsulation efficiency percentage (EE%) of Chr within the NPs, specific formulas were applied.

$$DL\% = \left(\frac{Weight\ of\ drug\ in\ NPs}{Total\ weight\ of\ NPs}\right) \times 100 \tag{1}$$

$$EE\% = \left(\frac{Weight\ of\ drug\ in\ NPs}{Initial\ weight\ of\ drug\ used\ for\ loading}\right) \times 100$$
(2)

2.4 Characterization of NPs

The Au/CS NPs' hydrodynamic diameter, distribution of particle size, and zeta potential were measured using a Nano/zetasizer (from Malvern Instruments, Nano ZS, Worcestershire, UK) which employs the dynamic light scattering (DLS) technique. The nanostructure's physical stability was gauged by observing its size and zeta potential over a span of a month. Its crystalline form was discerned using a Bruker D8Advence XRD that uses Cu $K\alpha$ radiation (k = 1.5418 A) and operates at settings of 40 kV and 30 mA. Visual representations of the Au/CS NPs' morphology were captured using transmission electron microscopy (TEM; sourced from Zeiss, set at 80 KeV, model EM 900) and scanning electron microscopy (SEM; model Mira 3-XMU, at 700 kV). The FT-IR spectra, spanning a range of 400–4000 cm⁻¹, were acquired on an FT-IR spectrophotometer (from Matson) using KBr plates.

2.5 In vitro drug release study

The release behavior of Chr from the Au/CS NPs was examined in PBS with 0.5% w/v Tween 80, both at a physiological pH of 7.4 and in a more acidic environment with a pH of 5.4. Typically, 2.0 ml of the Au/CS NPs were secured within a dialysis bag (with a cut-off at 12 kDa) by sealing its ends with clamps. This bag was then immersed in 13 ml of PBS at the chosen pH, continuously stirred at a rate of 100 rpm and maintained at a temperature of 37 °C. At specific time points, 1.0 ml of the surrounding solution was sampled to gauge the drug's release amount, and immediately replenished with an equivalent volume of fresh buffer under the same conditions. The concentration of the curcumin in these samples was ascertained using UV-Vis spectroscopy, focusing on a 267 nm wavelength.



2.6 Radical scavenging activity of the Chr@Au/CS NPs

The capacity of Chr-Au/CS NPs to neutralize free radicals was evaluated using 2, 2-diphenyl-2-picrylhydrazyl (DPPH). In a summarized procedure, both Chr and Chr-Au/CS NPs, dissolved in methanol at concentrations ranging from 0.006 to 0.06 mM, were mixed with 1 ml of a 0.2 mM DPPH radical solution in methanol. This mixture was then shaken intensively and left in the dark for varying durations (10, 20, and 30 minutes) prior to recording its absorbance at 517 nm. The scavenging capacity was computed using a subsequent equation.

DPPH radical scavenging (%) =
$$\frac{Ac - As}{Ac} \times 100$$
 (3)

where, Ac stands for the absorbance of the blank, and As indicates the absorbance of the sample.

2.7 MTT assay

The viability of MDA-MB-231 breast cancer cells in response to the introduced nanogels was examined using the MTT colorimetric assay. In brief, these cells were grown in RPMI-1640, supplemented with 1% penicillin/Streptomycin and 10% FBS. They were then housed in a cell culture incubator that maintained a physiological temperature of 37 °C, in a humid environment with 5% CO₂. For testing, cells were allocated to 96-well plates at a density of 10,000 cells per well 24 hours before treatment. These cells were then exposed to escalating doses (ranging from 30 to 240 µuM) of standalone Chr, the formulated Chr-Au/CS NPs, and just the Au/CS NPs. After a 72-hour treatment period, cell survival was gauged using the MTT colorimetric technique. Specifically, each well received 20 μ L of an MTT solution (concentration: 5 mg/ml in PBS), and the plate underwent a 4-hour incubation in the aforementioned CO2 incubator. Subsequent to this, the medium was discarded, formazan crystals were dissolved in 100 μ L DMSO, and absorbance was determined using a plate reader, set to 570 nm with a reference wavelength of 690 nm. The percentage of viable cells was determined relative to a control group.

2.8 Statistics

Data was analyzed using the GraphPad Prism software (version 9). A One-Way ANOVA was employed, and the means of the groups were compared using the Tukey posthoc test. Results with a P value of 0.05 or less were deemed statistically significant.

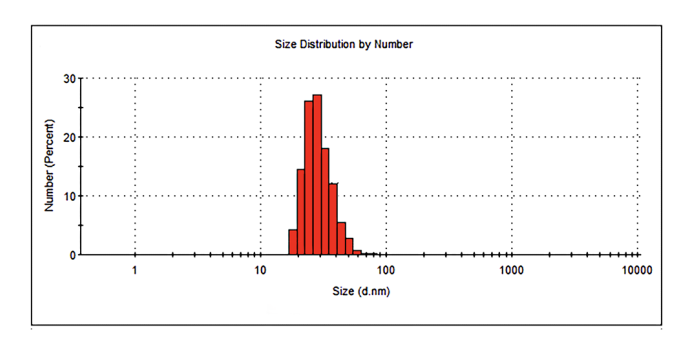
3 RESULTS AND DISCUSSION

3.1 Preparation and characterization of the NPs

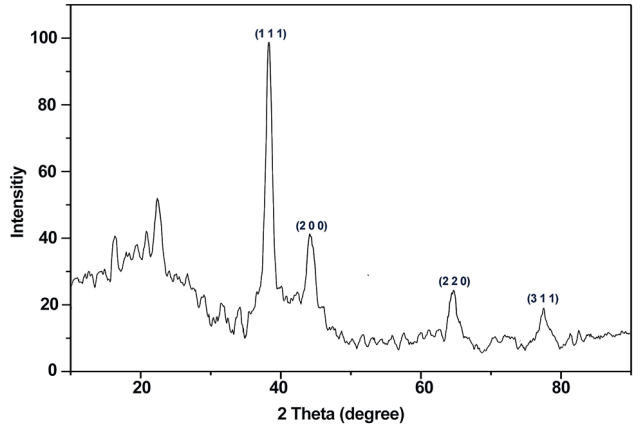
To enhance the water solubility of Chr and prolong its stay at the targeted biological site through the EPR effect, Au/CS NPs were synthesized. The initial step involved creating ion pairs between $AuCl_4^-$ and positively charged chitosan, which acted as both a reducing and stabilizing agent. It's been established that the degree of interaction between $AuCl_4^-$ and chitosan's amino groups significantly dictates the size of AuNPs. TPP, known for its ability to form ionic bonds with CS, is a prevalent choice for crafting CS NPs. This technique is both gentle and effective, catering to various therapeutic needs. Moreover, TPP contributes to the generation of smaller-sized AuNPs [13, 14].

The NPs' mean size and their associated polydispersity index (PDI) were found to be 45.23 ± 4.32 nm and 0.21 ± 0.05 , as shown in Fig.1a. The X-ray diffraction pattern, represented in Fig.1b, displayed distinctive peaks at (1 1 1), (2 0 0), (2 2 0), and (3 1 1) Bragg reflections, corroborating the crystalline nature of the AuNPs-a finding consistent with prior research [15].

TEM and FE-SEM imaging, depicted in Fig.1c and 1d, respectively, confirm that the developed Au/CS NPs are nearly spherical, averaging around 42 nm in size.



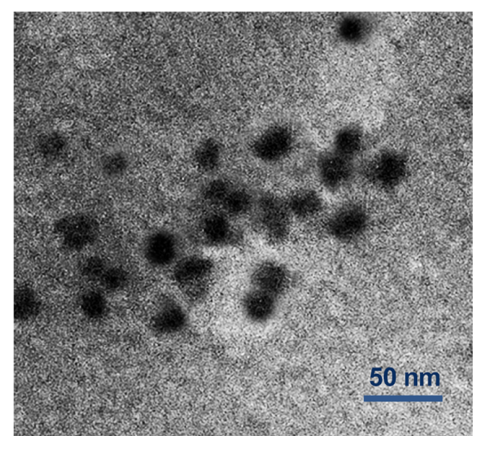
(a) The DLS particles size distribution



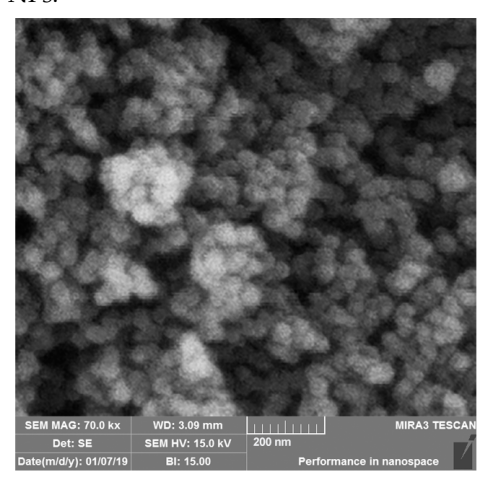
(b) The X-ray diffraction patterns.

Fig. 1. Characterization of the Au/CS NPs.





(c) FE-SEM and TEM images of the Au/CS NPs.



(d) The DLS particles size distribution

Fig. 1. Characterization of the Au/CS NPs.

Figure 2 showcases the FT-IR spectrum for CS, Au/CS NPs, and Chr-Au/CS NPs. In the CS spectrum, the 3446 cm⁻¹ absorption band relates to the –OH stretching vibration. Bands at 1600 cm⁻¹ and 1392 cm⁻¹ are linked to CS's primary chain formed by N-H and CH2 stretching vibrations [16]. For the Au/CS NPs, the absorption bands emerging at 3430 cm⁻¹, 1591 cm⁻¹, and 1412 cm⁻¹ can be associated with O-H, N-H, and CH2 groups of CS, respectively [17]. A notable peak at 1068 cm⁻¹ signifies the P=O bond presence in TPP, pointing to the CS NPs' formation. Peaks at 1500 cm⁻¹ and 1706 cm⁻¹ correspond to the C-C bond in the aromatic ring and the carbonyl group in Chr's composition, suggesting successful drug encapsulation within the NPs.

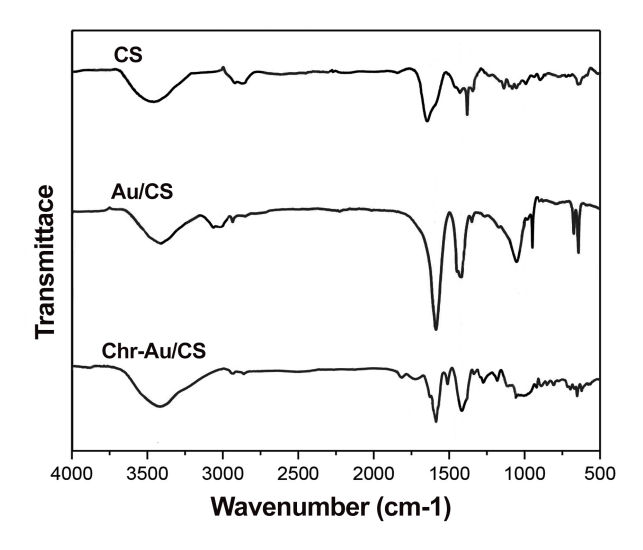


Fig. 2. FT-IR spectra of CS, Au/CS NPs and Chr-Au/CS NPs.

3.2 Drug loading and in vitro drug release

The findings indicate that the drug loading and encapsulation effectiveness of the Au/CS NPs for Chr stood at 20 \pm 3.70% and 88.70 \pm 4.5%, respectively. This elevated drug loading capacity may be attributed to the robust hydrogen bonding between the -OH groups present in CS and the structure of Chr. Fig.3 displays the drug's release pattern from the Au/CS NPs in PBS, observed at two distinct pH levels (5.4 and 7.4) maintained at a body temperature of 37 °C. These curves represent the ongoing release of Chr from the nanoparticles. Notably, there's a pronounced immediate release in the initial 24 hours, especially at pH levels of 7.4 and 5.3. The drug's release rate in acidic conditions was almost double than in a neutral setting, highlighting the pH-responsive nature of the carrier, likely due to the presence of CS [18]. These characteristics of drug release make this carrier suitable for applications as a responsive drug nanocarrier.

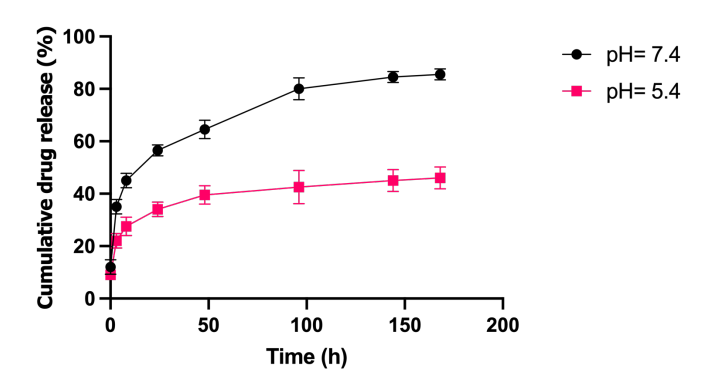


Fig. 3. Drug release behavior of Au/CS NPs at two different pH.



3.3 Antioxidant activity

The anticancer properties of Chr are largely attributed to its robust antioxidant and free-radical neutralizing capacities. The antioxidant abilities of both Chr and Chr-Au/CS NPs were assessed using the DPPH scavenging method. DPPH serves as a stable lipophilic free radical benchmark commonly employed to test the radical-neutralizing potential of organic substances [19]. As depicted in Fig.4, noticeable disparities were seen between the results for unbound Chr and the Chr-Au/CS NPs. As the concentration of Chr escalated, the antioxidant efficacy of both forms also heightened. Understandably, the Chr-embedded Au/CS NPs exhibited diminished antioxidant prowess relative to the standalone Chr, likely due to the controlled release mechanism of Chr from the nanoparticles.

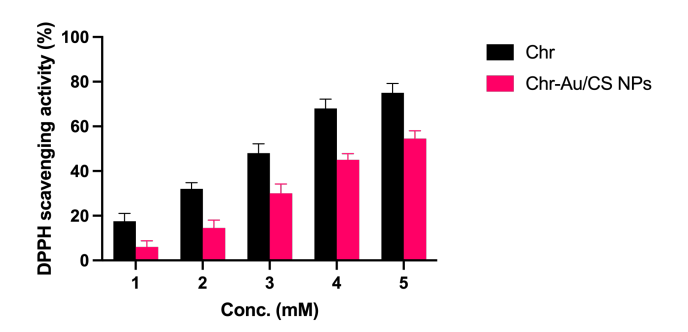


Fig. 4. DPPH radical scavenging activity of the free Chr and Chr loaded Au/CS NPs.

3.4 Cytotoxicity

The suppressive potential of Chr-Au/CS NPs was examined on MDA-MB-231 cells, which are characterized as highly aggressive, invasive, and undifferentiated triplenegative breast cancer cells. The outcomes from the MTT survival tests on these cells are shown in Fig.5. During the 72-hour study, cells underwent treatment with escalating doses of Chr-Au/CS NPs, undocked NPs, and unencapsulated Chr. The Chr concentration in the Chr-Au/CS NPs was adjusted based on drug load capacity. Notably, the cytotoxicity exhibited by the Chr-infused nanoparticles was markedly greater than that of independent Chr. After a 72-hour contact with the Chr-enriched Au/CS NPs, the IC50 was computed to be 32.3 μ M, nearly half of the value found for the isolated curcumin, which had an IC50 of approximately 58.5 µM. This heightened effectiveness is likely due to the enhanced solubility and superior cellular uptake of the Au/CS NPs when contrasted with free Chr. In essence, the findings suggest that this NPs formulation bolsters the anticancer potency of Chr. Additionally, even at elevated concentrations, Au/CS NPs showcased minimal cytotoxic effects, emphasizing their potential safety as a nanocarrier.

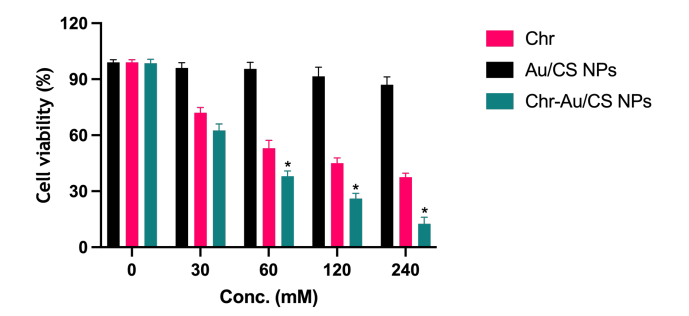


Fig. 5. The cytotoxicity of the Chr-Au/CS NPs on MDA-MB-231 cells. The cells were treated with the desired concentration of samples and incubated for 72 h at cell culture incubator. Cell viability was then assessed using MTT method. Cell viability was presented as ratio (%) to control group.*P \leq 0.05.

4 CONCLUSION

The study successfully fabricated Au/CS NPs with the primary aim of enhancing the aqueous solubility and biological retention of Chr. Utilizing the inherent properties of chitosan and TPP, the formulated NPs exhibited an average size of approximately 42-45 nm with a crystalline structure confirmed by characteristic Bragg reflections. Infrared spectra further elucidated the structural characteristics of the NPs, highlighting successful drug entrapment evidenced by specific peaks relating to chrysin's structure.

Notably, the drug loading capacity of these NPs for Chr was observed to be high, potentially due to the strong hydrogen bonds formed between chitosan and chrysin. This high drug loading coupled with the drug release profile, particularly the pH sensitivity of the carrier due to chitosan, positions the Au/CS NPs as a promising candidate for use as a triggered drug nanocarrier.

From an application perspective, the superior antioxidant potential of free Chr was evident. However, Chr-loaded Au/CS NPs demonstrated a more potent cytotoxic effect against MD-MBA-231 breast cancer cells compared to free Chr. Specifically, the IC50 value for Chr-loaded NPs was nearly half of that for free Chr, underscoring the enhanced solubility and cell penetration abilities of the Au/CS NPs. The comparatively low cytotoxic nature of the Au/CS NPs even at higher concentrations also underscores its potential as a safe and effective nanocarrier.

Conflict of Interest: The authors declare no conflict of interest.

Financing: The study was performed without external funding.

Ethical consideration: The study was approved by University of Wasit, Wasit, Iraq.



REFERENCES

- [1] Dey S, Sherly MCD, Rekha M, Sreenivasan K. Alginate stabilized gold nanoparticle as multidrug carrier: Evaluation of cellular interactions and hemolytic potential. Carbohydrate polymers. 2016;136:71-80. doi:10.1016/j.carbpol.2015.09.016.
- [2] Talebi M, Talebi M, Farkhondeh T, Simal-Gandara J, Kopustinskiene DM, Bernatoniene J, et al. Emerging cellular and molecular mechanisms underlying anticancer indications of chrysin. Cancer Cell International. 2021;21(1):1-20. doi:10.1186/s12935-021-01906y.
- [3] Shahbaz M, Naeem H, Imran M, Ul Hassan H, Alsagaby SA, Al Abdulmonem W, et al. Chrysin a promising anticancer agent: recent perspectives. International Journal of Food Properties. 2023;26(1):2294-337. doi:10.1080/10942912.2023.2246678.
- [4] Narvekar M, Xue HY, Eoh JY, Wong HL. Nanocarrier for poorly water-soluble anticancer drugs—barriers of translation and solutions. Aaps Pharmscitech. 2014;15:822-33. doi:10.1208/s12249-014-0107-x.
- [5] Ganai SA, Sheikh FA, Baba ZA. Plant flavone Chrysin as an emerging histone deacetylase inhibitor for prosperous epigenetic-based anticancer therapy. Phytotherapy Research. 2021;35(2):823-34. doi:10.1002/ptr.6869.
- [6] Nejati K, Dadashpour M, Gharibi T, Mellatyar H, Akbarzadeh A. Biomedical applications of functionalized gold nanoparticles: a review. Journal of Cluster Science. 2021;33:1-16. doi:10.1007/s10876-020-01955-9.
- [7] D'Acunto M, Cioni P, Gabellieri E, Presciuttini G. Exploiting gold nanoparticles for diagnosis and cancer treatments. Nanotechnology. 2021;32(19):192001. doi:10.1088/1361-6528/abe1ed.
- [8] Shaabani E, Sharifiaghdam M, De Keersmaecker H, De Rycke R, De Smedt S, Faridi-Majidi R, et al. Layer by layer assembled chitosan-coated gold nanoparticles for enhanced siRNA delivery and silencing. International journal of molecular sciences. 2021;22(2):831. doi:10.3390/ijms22020831.
- [9] Labala S, Jose A, Venuganti VVK. Transcutaneous iontophoretic delivery of STAT3 siRNA using layerby-layer chitosan coated gold nanoparticles to treat melanoma. Colloids and Surfaces B: Biointerfaces. 2016;146:188-97. doi:10.1016/j.colsurfb.2016.05.076.
- [10] Bhumkar DR, Joshi HM, Sastry M, Pokharkar VB. Chitosan reduced gold nanoparticles as novel carriers

- for transmucosal delivery of insulin. Pharmaceutical research. 2007;24:1415-26. doi:10.1007/s11095-007-9257-9.
- [11] Stobiecka M, Hepel M. Double-shell gold nanoparticle-based DNA-carriers with poly-L-lysine binding surface. Biomaterials. 2011;32(12):3312-21. doi:10.1016/j.biomaterials.2010.12.064.
- [12] Amanlou N, Parsa M, Rostamizadeh K, Sadighian S, Moghaddam F. Enhanced cytotoxic activity of curcumin on cancer cell lines by incorporating into gold/chitosan nanogels. Materials chemistry and physics. 2019;226:151-7. doi:10.1016/j.matchemphys.2018.12.089.
- [13] Doudna JA. The promise and challenge of therapeutic genome editing. Nature. 2020;578(7794):229-36. doi:10.1038/s41586-020-1978-5.
- [14] Zhu F, Chen G, Sun S, Sun X. In situ growth of Au@ CeO 2 core–shell nanoparticles and CeO 2 nanotubes from Ce (OH) CO 3 nanorods. Journal of Materials Chemistry A. 2013;1(2):288-94. doi:10.1039/C2TA00293K.
- [15] Dong Y, Gao T, Zhou Y, Chu X, Wang C. Enhancement of electrogenerated chemiluminescence of luminol by ascorbic acid at gold nanoparticle/graphene modified glassy carbon electrode. Spectrochimica Acta Part A: Molecular and Biomolecular Spectroscopy. 2015;134:225-32. doi:10.1016/j.saa.2014.06.117.
- [16] Kiechel MA, Schauer CL. Non-covalent crosslinkers for electrospun chitosan fibers. Carbohydrate polymers. 2013;95(1):123-33. doi:10.1016/j.carbpol.2013.02.034.
- [17] Chung TW, Chang CH, Ho CW. Incorporating chitosan (CS) and TPP into silk fibroin (SF) in fabricating spray-dried microparticles prolongs the release of a hydrophilic drug. Journal of the Taiwan Institute of Chemical Engineers. 2011;42(4):592-7. doi:10.1016/j.jtice.2010.11.003.
- [18] Khan MA, Zafaryab M, Mehdi SH, Ahmad I, Rizvi MMA. Characterization and anti-proliferative activity of curcumin loaded chitosan nanoparticles in cervical cancer. International journal of biological macromolecules. 2016;93:242-53. doi:10.1016/j.ijbiomac.2016.08.050.
- [19] Blois MS. Antioxidant determinations by the use of a stable free radical. Nature. 1958;181(4617):1199-200. doi:10.1038/1811199a0.



How to cite this article

Dilfy S.H.; Mubark N.N.; Ahad A.; Optimizing Chrysin's Anticancer Efficacy on MDA-MB-231 Cells: Synthesis and Characterization of Chrysin-Loaded Gold/Chitosan Nanoparticles. Trends in Pharmaceutical Biotechnology (TPB). 2023;1(1):12-18. doi: 10.57238/tpb.2023.144270.1001

